

LETTERS

Rovibrationally Selected and Resolved Pulsed Field Ionization-Photoelectron Study of Ethylene

Peng Wang, Xi Xing, Sun Jong Baek, and C. Y. Ng*

*Department of Chemistry, University of California, Davis, One Shields Avenue, Davis, California 95616**Received: August 9, 2004; In Final Form: October 7, 2004*

We show that by preparing ethylene (C_2H_4) in selected rotational levels of the C–H stretching $\nu_9(b_{2u}) = 1$ or $\nu_{11}(b_{1u}) = 1$ state by infrared (IR) laser excitation prior to vacuum ultraviolet (VUV) laser photoionization, greatly simplified, rotationally resolved pulsed field ionization-photoelectron spectra can be obtained, leading to reliable rotational assignments of the vibrational bands for $C_2H_4^+(\tilde{X}^2B_{3u}; \nu_4^+(\text{torsional}) = 1 \text{ or } \nu_{11}^+ = 1) \leftarrow C_2H_4(\tilde{X}^1A_g; \nu_{11} = 1)$ and $C_2H_4^+(\tilde{X}^2B_{3u}; 0^{0+}) \leftarrow C_2H_4(\tilde{X}^1A_g; \nu_9 = 1)$. The observation of these Franck–Condon (FC) forbidden vibrational bands is indicative of a strong state-mixing mechanism, in which Rydberg states converging to the FC forbidden $C_2H_4^+(\tilde{X}^2B_{3u}; 0^{0+}$ and $\nu_4^+ = 1)$ levels are effectively coupled via intermediate states to Rydberg levels converging to FC allowed $C_2H_4^+(\tilde{X}^2B_{3u}; \nu_9^+ = 1$ and $\nu_{11}^+ = 1)$ states, respectively. This conclusion is supported by strong autoionizing features observed in the IR–VUV photoionization efficiency spectra.

With the recent improvement in energy resolution,^{1,2} the vacuum ultraviolet (VUV)-pulsed field ionization-photoelectron (VUV–PFI–PE) method has become a major technique for the study of ion spectroscopy and photoionization dynamics. However, as its application expands to include larger polyatomic molecules, it will undoubtedly encounter the common problem of spectral congestion that could prevent the rotational assignment of the PFI–PE spectrum. It is well-known that this problem can be alleviated by reducing the initial populations of excited rovibrational levels by lowering the temperature of the gas sample by using techniques such as the supersonic expansion³ and the helium droplet⁴ methods. An ideal spectroscopic experiment can be designed by preparing the molecules of interest in a single, selected rovibrational state by IR laser excitation prior to spectroscopic investigation.

A rovibrationally selected IR–VUV-photoionization efficiency (IR–VUV–PIE) study of acetylene has been made

recently using VUV synchrotron radiation and an IR laser.⁵ However, the mismatch of the repetition rates for the IR laser and the pseudo-continuum VUV synchrotron source proves the combination inefficient for IR–VUV studies. We have recently demonstrated a vibrationally selected and resolved IR–VUV–PFI–PE study of trichloroethene using IR and VUV lasers.⁶ This communication reports the first rovibrationally state-resolved VUV–PFI–PE study of C_2H_4 prepared in selected rovibrational levels of the C–H stretching modes [$\nu_9(b_{2u}) = 3105.3 \text{ cm}^{-1}$ and $\nu_{11}(b_{1u}) = 2989.1 \text{ cm}^{-1}$]⁷ by IR laser excitation. In the recent VUV–PFI–PE study of C_2H_4 in its ground state prepared in a supersonic beam, Merkt and co-workers have reported detailed rotational-analyses of observed vibrational bands of $C_2H_4^+(\tilde{X}^2B_{3u})$.¹ They point out that a PFI–PE resolution of 0.09 cm^{-1} (fwhm) is required to clearly resolve the rotational structure of the $C_2H_4^+[\tilde{X}^2B_{3u}; \nu_4^+(\text{torsional})]$ bands. As shown below, by selecting a rotational level of $C_2H_4(\tilde{X}^1A_g; \nu_9 = 1 \text{ or } \nu_{11} = 1)$ prior to VUV photoionization, rotational structures of the IR–VUV–PFI–PE spectra can be

* To whom correspondence should be addressed. Electronic mail: cying@chem.ucdavis.edu.

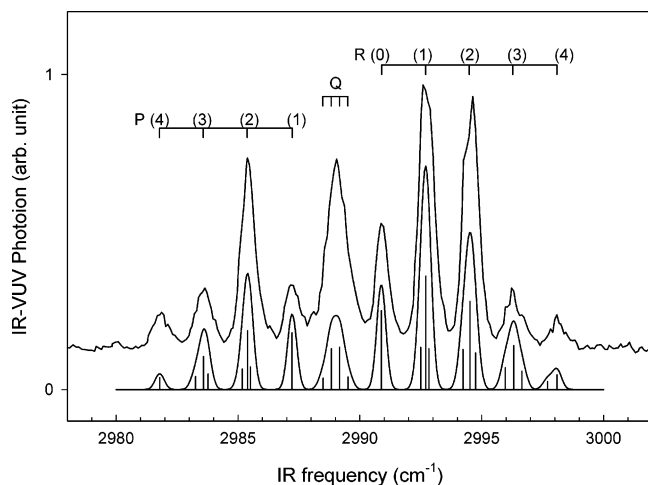


Figure 1. IR–VUV-photoion spectrum of $C_2H_4(\nu_{11} = 1)$ in the IR range of 2978–3002 cm^{-1} . The P(1) and R(1) transitions are selected for IR–VUV measurements. The positions and relative intensities of the $N_{K_aK_c}$ rotational levels are shown as vertical sticks in the simulated spectrum, where individual peaks are resulted from overlapping $N_{K_aK_c}$ levels.

adequately resolved and assigned using a resolution more than 10-fold lower than that used in ref 1. Furthermore, state-to-state photoionization cross sections obtained in the present study have provided insight into the couplings of different vibrational modes induced by threshold photoionization. Due to different selection rules, the VUV–PFI–PE study of ref 1 and the present IR–VUV–PFI–PE study can be considered as complementary.

The procedures for single-photon VUV and two-color IR–VUV PIE and PFI–PE measurements using the IR–VUV laser photoion-photoelectron apparatus have been described previously.^{6,8} Briefly, tunable VUV laser radiation (30 Hz) is generated by resonant enhanced four-wave difference-frequency mixing in a Kr gas cell using the $5p'[0(1/2),0] \leftarrow 4p^6$ two photon resonance at 98 855.1 cm^{-1} , and selected by a windowless VUV monochromator. The IR laser radiation is generated by an optical parametric oscillator/amplifier pumped by an Nd:YAG laser (15 Hz). The typical IR pulse energy at the 3 μm region is ≈ 5 mJ/pulse with an optical bandwidth of ≈ 0.3 cm^{-1} (fwhm). Because the repetition rate of the VUV laser is twice that of the IR laser, shot-to-shot subtraction of the VUV-only background is possible. However, no shot-to-shot subtraction was performed for the present experiment. The VUV laser and the C_2H_4 beam intersect perpendicularly at the photoionization region. The IR beam is aligned counter-propagating with the VUV beam. In IR–VUV measurement, the VUV laser pulse is delayed ≈ 20 –50 ns with respect to the IR laser pulse. The C_2H_4 (purity = 99.95%) sample is premixed with He in the 1:9 ratio to a total stagnation pressure of 1.5 atm prior to entering the photoionization region as a skimmed pulsed beam (30 Hz).

The IR photoion spectrum of the $C_2H_4(\nu_{11} = 1)$ band obtained by scanning the IR laser frequency in the range of 2978–3002 cm^{-1} with the VUV frequency fixed at 84 731 cm^{-1} is depicted in Figure 1 (upper spectrum). The best simulated spectrum of this band obtained using known rotational constants⁷ of C_2H_4 [$A = 4.8646064(17)$ cm^{-1} , $B = 1.0010545(5)$ cm^{-1} , and $C = 0.8280424(4)$ cm^{-1}] and an instrumental Gaussian profile [full-width at half-maximum (fwhm) = 0.22 cm^{-1}] is shown as the lower spectrum in Figure 1. The simulation gives: $\nu_{11} = 2989.1$ cm^{-1} and rotational temperature of $C_2H_4 = 8$ K.⁷ The rotational transitions P(1) and R(1) are chosen for IR–VUV–PIE and IR–VUV–PFI–PE measurements. Though P(1) corresponds only to the 0_{00} rotational state, R(1) consists of three

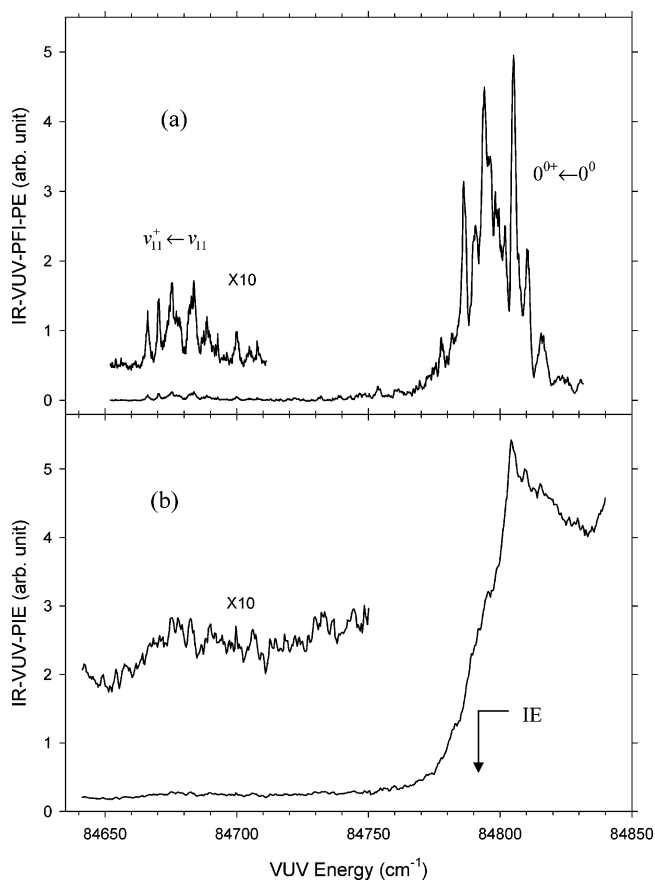


Figure 2. Comparison of the (a) IR–VUV–PFI–PE and (b) IR–VUV–PIE spectra for C_2H_4 in the VUV range of 84 635–84 850 cm^{-1} obtained with the IR laser frequency set at R(1) of the ν_{11} band.

main rotational states, 2_{02} , 2_{12} , and 2_{11} of $C_2H_4(\nu_{11} = 1)$. Here, the rotational level for C_2H_4 ($C_2H_4^+$) is designated as $N_{K_aK_c}(N^+K_a^+K_c^+)$, where N (N^+) represents the total angular momentum quantum number without spin, and $K_a(K_a^+)$ and $K_c(K_c^+)$ are the asymmetric top quantum numbers of the neutral (ion). The positions and relative intensities of the $N_{K_aK_c}$ rotational levels for $C_2H_4(\nu_{11} = 1)$ are shown as vertical sticks in the simulated spectrum, where individual peaks result from overlapping $N_{K_aK_c}$ levels. As shown in Figure 1, the observed intensities of the P(2), Q, and R(2) peaks of the experimental spectrum are higher than the corresponding peaks of the simulated spectrum. This discrepancy can be attributed to different photoionization cross sections for the $N_{K_aK_c}$ rotational levels at the fixed VUV frequency. Because 2_{02} is at the central maximum of R(1), it is the most populous state. A similar IR photoion spectrum (not shown here) is obtained for the $\nu_9 = 1$ band, in which R(1) (mainly consists of two rotational states 2_{21} and 2_{20}) is selected for IR–VUV measurements.

Parts a and b of Figure 2a,b compare the IR–VUV–PFI–PE and IR–VUV–PIE spectra for C_2H_4 ($\nu_{11} = 1$) in the VUV region of 84 640–84 840 cm^{-1} obtained by setting the IR laser frequency at R(1) of Figure 1. The dominant PFI–PE band of Figure 2a is identified as the origin band of $C_2H_4^+(\tilde{X}^2B_{3u}; 0^0_+)$ and the prominent PIE step of Figure 2b manifests the corresponding ionization onset of C_2H_4 by VUV only photoionization. These structures are essentially unaffected by the IR laser. The PFI–PE and PIE intensities observed at VUV energies below these prominent structures are $< 2.5\%$ and $< 5\%$ of the respective intensities of the VUV–PFI–PE origin band and VUV–PIE step and are identified to result from IR–VUV photoionization. The low IR–VUV–PIE and

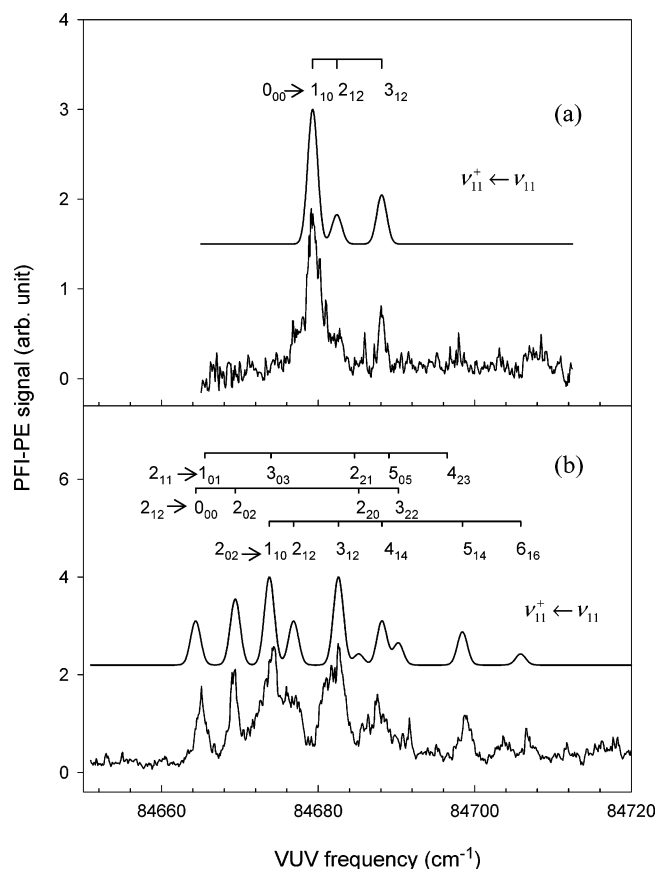


Figure 3. IR–VUV–PFI–PE spectra (lower curves) for C_2H_4 with the IR laser frequency set at (a) P(1) and (b) R(1). The upper curves represent the best-fit spectra. The rotational assignments ($N_{K_a K_c} \rightarrow N^+_{K_a^+ K_c^+}$) are marked on top of the figure.

IR–VUV–PFI–PE intensities indicate either that only a small fraction of C_2H_4 molecules in the molecular beam are excited by the IR laser or that the VUV photoionization cross sections of $C_2H_4(\tilde{X}^1A_g; \nu_9 = 1$ or $\nu_{11} = 1)$ are very low near the ionization threshold. The fact that we cannot obtain a VUV–PFI–PE depletion spectrum⁶ [with the VUV set at the IE(C_2H_4)] with good signal-to-noise ratios as the IR is scanned through the $\nu_9 = 1$ and $\nu_{11} = 1$ bands is indicative of low IR absorption.

Despite the low IR–VUV–PFI–PE intensity, rotationally resolved IR–VUV–PFI–PE vibrational bands can be observed as illustrated in the magnified spectrum in Figure 2a, which is also plotted in Figure 3b (lower spectrum) for comparison with the IR–VUV–PFI–PE spectrum of Figure 3a (lower spectrum) observed by setting the IR laser frequency at P(1) of the ν_{11} band. The appearance of this IR–VUV–PFI–PE band corresponds to a step in the IR–VUV–PIE spectrum (see the magnified spectrum in Figure 2b). Considering that the photoionization of C_2H_4 involves the removal of an electron from the C=C bond, we do not expect the C–H bonds to be seriously affected. That is, the formation of $C_2H_4^+(\nu_{11}^+)$ from $C_2H_4(\nu_{11})$ should be efficient. Because the experimental frequency for ν_{11}^+ (b_{1u}) is not known, we have calculated the harmonic frequencies for C_2H_4 and $C_2H_4^+$ at the B3LYP/6-311++G(2df,p) level of theory.⁹ Comparing the calculated harmonic frequency of 3124 cm^{-1} with the experimental frequency of 2989.1 cm^{-1} for $\nu_{11}(b_{1u})$, we obtained a scaling factor of 0.957 for the theoretical frequency. Applying this scaling factor to the theoretical frequency of 3084 cm^{-1} for $\nu_{11}^+(b_{1u})$, we obtain the prediction of $\nu_{11}^+(b_{1u}) = 2951\text{ cm}^{-1}$.

The latter value predicts that the $\nu_{11}^+ \leftarrow \nu_{11}$ band occurs $\approx 40\text{ cm}^{-1}$ below the IE(C_2H_4) compared to the energy of $\approx 120\text{ cm}^{-1}$ below the IE(C_2H_4) for the IR–VUV–PFI–PE band of Figure 3a,b. Without further theoretical and experimental information, we tentatively assign this band to the $\nu_{11}^+ \leftarrow \nu_{11}$ transition.

In the case of ethylene (D_{2h}), the general rovibronic symmetry selection rule for photoionization transitions^{1,10} is $\Gamma_e^+ \otimes \Gamma_v^+ \otimes \Gamma_r^+ \otimes \Gamma_e^- \otimes \Gamma_v^- \otimes \Gamma_r^- \supset A_u$, where Γ_e^+ , Γ_v^+ , and Γ_r^+ (Γ_e^- , Γ_v^- , and Γ_r^-) represent the respective electronic, vibrational, and rotational symmetries of the ionic (neutral) states, and Γ_e^- is the symmetry of the photoelectron, which can be either A_g or A_u , depending on whether the photoelectron orbital angular momentum l is even (e) or odd (o). Assuming the transition to be $C_2H_4^+(\tilde{X}^2B_{3u}; \nu_{11}^+, N^+_{K_a^+ K_c^+}) \leftarrow C_2H_4(\tilde{X}^1A_g; \nu_{11}, N_{K_a K_c})$, we have $\Gamma_e = A_g$, $\Gamma_e^+ = B_{3u}$, and both Γ_v and Γ_v^+ are B_{1u} . The rotational symmetry $\Gamma_r(\Gamma_r^+)$ depends on K_a (K_a^+) and K_c (K_c^+). For $K_a K_c = ee, eo, oe, \text{ and } oo$, $\Gamma_r = A_g, B_{1g}, B_{3g}, \text{ and } B_{2g}$, respectively. Because rotational symmetries are always g (gerade) in this case, the parity of l is determined by vibrational symmetries. The symmetry selection rule requires that l is even and $\Gamma_r^+ \otimes \Gamma_r \supset B_{3g}$. These requirements correspond to $\Delta K_a = K_a^+ - K_a = \text{odd}$ and $\Delta K_c = K_c^+ - K_c = \text{even}$. The identification of the ΔK_a and ΔK_c transitions of a PFI–PE band would help to assign the final vibrational mode symmetry of the $C_2H_4^+(\tilde{X}^2B_{3u})$ ion.

Using the rigid rotor rotational Hamiltonians for both the neutral and ionic states and the known rotational constants for $C_2H_4(\tilde{X}^1A_g)$ (given above) and $C_2H_4^+(\tilde{X}^2B_{3u})$ [$A^+ = 4.770(16)\text{ cm}^{-1}$, $B^+ = 0.9252(49)\text{ cm}^{-1}$, and $C^+ = 0.7832(58)\text{ cm}^{-1}$],¹ IE(C_2H_4) = $84\,790.42(23)\text{ cm}^{-1}$,¹ and $\nu_{11} = 2989.1\text{ cm}^{-1}$,⁷ we have assigned the observed rotational transitions ($N_{K_a K_c} \rightarrow N^+_{K_a^+ K_c^+}$) as marked on top of Figure 3a,b. The fact that these rotational transitions are consistent with $\Delta K_a = \text{odd}$ and $\Delta K_c = \text{even}$ supports the assignment of the transition for the PFI–PE bands of Figure 3a,b. This assignment yields IE($\nu_{11}^+ \leftarrow \nu_{11}$) = $84\,674.0(2)\text{ cm}^{-1}$ or $\nu_{11}^+ = 2872.7\text{ cm}^{-1}$, which is 78 cm^{-1} lower than the theoretical prediction of 2951 cm^{-1} . To obtain better intensity estimates of individual rotational transitions, we have performed a fit to the IR–VUV–PFI–PE spectra based on the rotational assignments. The upper spectra of Figure 3a,b are the best fits to the respective IR–VUV–PFI–PE spectra of Figure 3a,b obtained using an instrumental Gaussian profile with a fwhm of 1.5 cm^{-1} . Minor discrepancies in peak widths and positions between the best fit and experimental IR–VUV–PFI–PE spectra can be attributed to autoionization perturbation.

The FCF calculation based on the harmonic approximation shows that the photoionization of $C_2H_4[\tilde{X}^1A_g; \nu_9 = 1$ ($\nu_{11} = 1$)] near the IR–VUV ionization threshold [equal to the difference between IE(C_2H_4) and $\nu_{11} = 2989.1\text{ cm}^{-1}$ ($\nu_9 = 3105.3\text{ cm}^{-1}$)] has negligible FCFs. Thus, direct photoionization is not expected to be important. Contrary to this expectation, IR–VUV–PIE and IR–VUV–PFI–PE signals at energies down to the IR–VUV ionization thresholds are observed.

Figure 4 parts a (lower spectrum) and b depict the respective IR–VUV–PFI–PE and IR–VUV–PIE spectra in the VUV range of $81\,856\text{--}81\,930\text{ cm}^{-1}$ with the IR frequency set at R(1) of the ν_{11} band. On the basis of the known position of the $\nu_4^+ = 1$ level,¹ we have assigned this IR–VUV–PFI–PE spectrum to the $\nu_4^+ = 1 \leftarrow \nu_{11} = 1$ transition with the rotational transitions marked on top of Figure 4a. These rotational transitions fulfill the selection rule for this vibrational transition requiring both ΔK_a and ΔK_c to be odd. The fact that $\Gamma_v^+(\nu_4^+ = 1) = A_u$ requires l to be even. The best fit to the IR–VUV–PFI–PE spectrum based on the assignment is also depicted as the upper

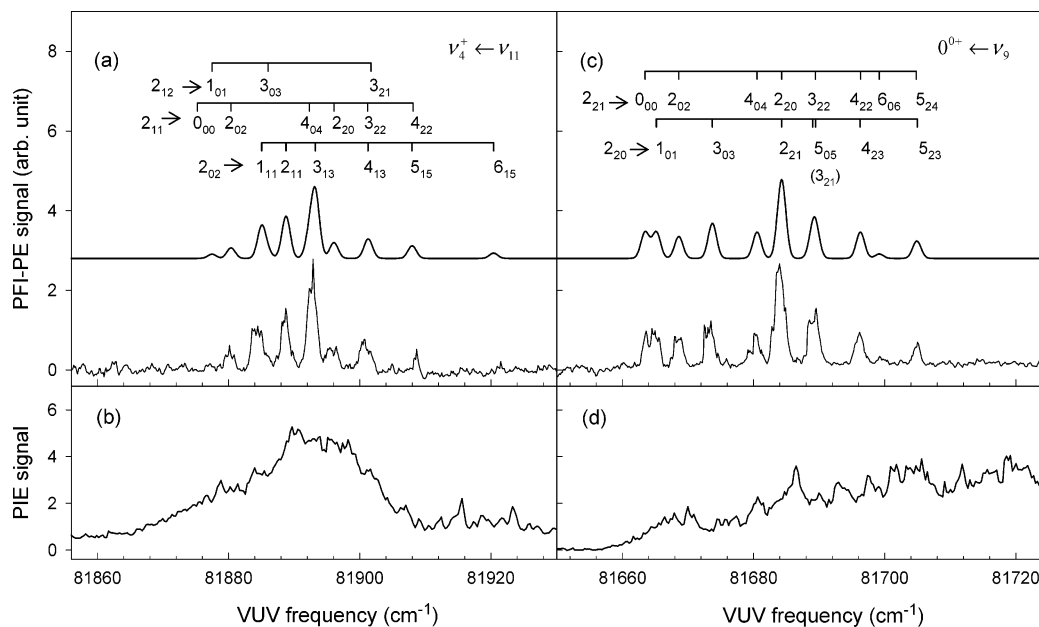


Figure 4. (a) and (b) are the respective IR–VUV–PFI–PE (lower curve) and IR–VUV–PIE spectra in the VUV region of 81 856–81 930 cm^{-1} observed by setting the IR laser frequency at R(1) of the ν_{11} band. (c) and (d) are respectively the IR–VUV–PFI–PE (lower curve) and IR–VUV–PIE spectra in the VUV region of 81 650–81 724 cm^{-1} observed by setting the IR laser frequency at R(1) of the ν_9 band. The upper curves of (a) and (c) represent the best fit spectra. The rotational assignments ($N_{K_a K_c} \rightarrow N_{K_a^+ K_c^+}$) are marked on top of (a) and (c).

spectrum in Figure 4a. Using the $\text{IE}(\text{C}_2\text{H}_4)^1$ $\nu_{11} = 2989.1 \text{ cm}^{-1}$,⁷ and $\text{IE}(\nu_4^+ = 1 \leftarrow \nu_{11} = 1) = 81\,885.4(2) \text{ cm}^{-1}$ determined here, we obtained $\nu_4^+ = 84.1 \text{ cm}^{-1}$, which is in accord with the known ν_4^+ value¹ of 83.7 cm^{-1} .

By setting the IR frequency at R(1) of the ν_9 band, we have also measured the IR–VUV–PFI–PE and IR–VUV–PIE spectra in the VUV region of 81 650–81 724 cm^{-1} as depicted in Figure 4 parts c (lower spectrum) and d, respectively. The ionization onset of these spectra indicates that the rotational transitions of Figure 4c belong to the $\text{C}_2\text{H}_4^+(\tilde{X}^2\text{B}_{3u}; 0^0+) \leftarrow \text{C}_2\text{H}_4(\tilde{X}^1\text{A}_g; \nu_9 = 1)$ vibrational band, satisfying the rotational selection rule $\Delta K_a = \text{even}$ and $\Delta K_c = \text{odd}$ as shown by rotational transitions marked at the top of Figure 4c. Here, $\Gamma_v(\nu_9 = 1) = \text{B}_{2u}$ and $\Gamma_v^+(0^0+) = \text{A}_g$ requires l to be odd. The best fit spectrum to the IR–VUV–PFI–PE spectrum obtained using an instrumentation Gaussian profile with a fwhm of 1.5 cm^{-1} is shown as the upper spectrum in Figure 4c. The assignment yields the $\text{IE}(0^0+ \leftarrow \nu_9 = 1) = 81\,685.3(2) \text{ cm}^{-1}$, which is consistent with the reported $\text{IE}(\text{C}_2\text{H}_4)$ value. As pointed above, the photoionization transitions $\nu_4^+ = 1 \leftarrow \nu_{11} = 1$ and $0^0+ \leftarrow \nu_9 = 1$ are not expected to be effective by direct photoionization on the basis of the FCF calculations. The observation of strong PFI–PE bands for these vibrational transition is consistent with an efficient state-mixing mechanism, in which Rydberg states converging to FC allowed excited vibrational states of the ion with $\nu_9^+ = 1$ and $\nu_{11}^+ = 1$ are strongly coupled via intermediate states to Rydberg states converging to FC forbidden 0^0+ and $\nu_4^+ = 1$ vibrational states of the ion. The dominant autoionization features observed in the IR–VUV–PIE spectra of Figure 4b,d are consistent with this mechanism. The fact that the maximum PFI–PE intensities observed in Figure 4a,c correlate with autoionizing PIE maxima for C_2H_4 exhibited in Figure 4b,d,

respectively, indicates that the PFI–PE intensities are mediated by intermediate autoionizing states. As a result, the simulation of the relative rotational PFI–PE intensities using the extended BOS model^{11,12} as in the single-photon VUV–PFI–PE study¹ of C_2H_4 is likely inappropriate because this model does not take into account inter-channel couplings, which are important for the state-mixing mechanism.

Acknowledgment. This work was partially supported by the USDOE Contract No. DE-FG02-02ER15306, AFOSR Grant No. F49620-03-1-0116, and NSF ATM 0317422.

References and Notes

- (1) Willitsch, S.; Hollenstein, U.; Merkt, F. *J. Chem. Phys.* **2004**, *120*, 1761.
- (2) Hollenstein, U.; Seiler, R.; Schmutz, H.; Andrist, M.; Merkt, F. *J. Chem. Phys.* **2001**, *115*, 5461.
- (3) Smalley, R. E.; Ramakrishna, B. L.; Levy, D. H.; Wharton, L. *J. Chem. Phys.* **1974**, *61*, 4363.
- (4) Toennies, J. P.; Vilesov, A. F. *Annu. Rev. Phys. Chem.* **1998**, *49*, 1.
- (5) Qian, X.-M.; Kung, A. H.; Zhang, T.; Lau, K. C.; Ng, C. Y. *Phys. Rev. Lett.* **2003**, *91*, 233001.
- (6) Woo, H. K.; Wang, P.; Lau, K. C.; Xing, X.; Chang, C.; Ng, C. Y. *J. Chem. Phys.* **2003**, *119*, 9333.
- (7) Martin, J. M. L.; Taylor, P. R. *Chem. Phys. Lett.* **1996**, *248*, 336.
- (8) Woo, H. K.; Lau, K.-C.; Zhan, J.-P.; Ng, C. Y.; Cheung, Y.-S.; Li, W. K.; Johnson, P. M. *J. Chem. Phys.* **2003**, *119*, 7789.
- (9) Frisch, M. J.; Trucks, G. W.; Schlegel, H. B. et al., *Gaussian 03*, revision B.5; Gaussian, Inc.: Pittsburgh, PA, 2003.
- (10) Signorelli, R.; Merkt, F. *Mol. Phys.* **1997**, *92*, 793.
- (11) Buckingham, A. D.; Orr, B. J.; Sichel, J. M. *Philos. Trans. R. Soc. London, Ser. A* **1970**, *268*, 147.
- (12) Wang, K.; McKoy, V. In *High-Resolution Laser Photoionization and Photoelectron Studies*; Power, I., Baer, T., Ng, C. Y., Eds.; Wiley: Chichester, 1995; pp 281–329.